

Accepted Manuscript

Development of the “hidden” multifunctional agents for Alzheimer's disease

Wenhai Huang, Meihao Liang, Qin Li, Xiaoliang Zheng, Chixiao Zhang, Qiao Wang, Li Tang, Zhimin Zhang, Beibei Wang, Zhengrong Shen



PII: S0223-5234(19)30461-1

DOI: <https://doi.org/10.1016/j.ejmech.2019.05.051>

Reference: EJMECH 11361

To appear in: *European Journal of Medicinal Chemistry*

Received Date: 19 March 2019

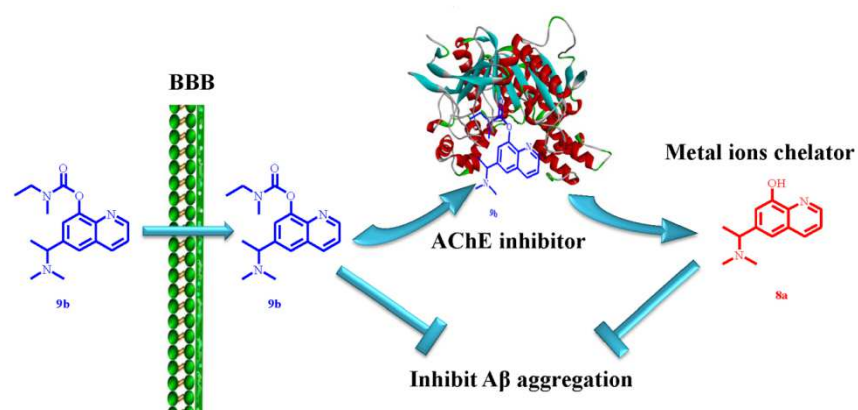
Revised Date: 26 April 2019

Accepted Date: 18 May 2019

Please cite this article as: W. Huang, M. Liang, Q. Li, X. Zheng, C. Zhang, Q. Wang, L. Tang, Z. Zhang, B. Wang, Z. Shen, Development of the “hidden” multifunctional agents for Alzheimer's disease, *European Journal of Medicinal Chemistry* (2019), doi: <https://doi.org/10.1016/j.ejmech.2019.05.051>.

This is a PDF file of an unedited manuscript that has been accepted for publication. As a service to our customers we are providing this early version of the manuscript. The manuscript will undergo copyediting, typesetting, and review of the resulting proof before it is published in its final form. Please note that during the production process errors may be discovered which could affect the content, and all legal disclaimers that apply to the journal pertain.

Graphical Abstract



Compound **9b** could cross the BBB efficiently and release **8a** into brain. **9b** had a potent AChE inhibitory activity, while **8a** displayed a significant metal ion chelating function, therefore in combination, both **9b** and **8a** exhibited a considerable inhibition of Aβ aggregation.

Development of the “hidden” multifunctional agents for Alzheimer’s disease

Wenhai Huang^{a,b}, Meihao Liang^a, Qin Li^a, Xiaoliang Zheng^c, Chixiao Zhang^a, Qiao Wang^a, Li Tang^{d,e}, Zhimin Zhang^a, Beibei Wang^a, Zhengrong Shen^{a,*}.

^aKey Laboratory of Neuropsychiatric Drug Research of Zhejiang Province, Institute of Materia Medica, Zhejiang Academy of Medical Sciences, Hangzhou 310013, PR China

^bState Key Laboratory of Medicinal Chemical Biology, Nankai University, Tianjin, PR China

^cCenter for Molecular Medicine, Zhejiang Academy of Medical Sciences, Hangzhou, P. R. China

^dDepartment of Pharmacy, School of Medicine, Health Science Center, Shenzhen University, Shenzhen, P. R. China.

^eNational-Regional Key Technology Engineering Laboratory for Synthetic Biology of Medicine, Shenzhen University, Shenzhen, P. R. China.

*Corresponding author: shenzr@zjams.com.cn, Tianmushan Road. NO.182, Zhejiang Academy of Medical Sciences, Hangzhou, 310013, P. R. China

Abstract: Alzheimer’s disease (AD) is a chronic, fatal and complex neurodegenerative disorder, which is characterized by cholinergic system dysregulation, metal dyshomeostasis, amyloid- β (A β) aggregation, etc. Therefore in most cases, single-target or single-functional agents are insufficient to achieve the desirable effect against AD. Multi-Target-Directed Ligand (MTDL), which is rationally designed to simultaneously hit multiple targets to improve the pharmacological profiles, has been developed as a promising approach for drug discovery against AD. To identify the multifunctional agents for AD, we developed an innovative method to successfully conceal the metal chelator into acetylcholinesterase (AChE) inhibitor. Briefly, the “hidden” agents first cross the Blood Brain Barrier (BBB) to inhibit the function of AChE, and the metal chelator will then be released via the enzymatic hydrolysis by AChE. Therefore, the AChE inhibitor, in this case, is not only a single-target agent against AD, but also a carrier of the metal chelator. In this study a total of 14 quinoline derivatives were synthesized and biologically evaluated. Both *in vitro* and *in vivo* results demonstrated that compound **9b** could cross the BBB efficiently, then release **8a**, the metabolite of **9b**, into brain. *In vitro*, **9b** had a potent AChE inhibitory activity, while **8a** displayed a significant metal ion chelating function, therefore in combination, both **9b** and **8a** exhibited a considerable inhibition of A β aggregation, one of the observations that plays important roles in the pathogenesis of AD. The efficacy of **9b** against AD was further investigated in both a zebrafish model and two different mice models.

Keywords: Alzheimer's disease; multifunctional agents; A β

ACCEPTED MANUSCRIPT

1. Introduction

Alzheimer's disease (AD), the leading cause of dementia in the elderly, is a chronic, fatal, and complex neurodegenerative disorder.^[1,2] In recent decades, only a few drugs were approved worldwide for treating AD. The failure rate of candidates in clinical trials is about 99.6% from 2002 to 2012, and particularly the failure of Solanezumab at phase III trial cast a shadow on the AD drug development.^[3] Since multiple factors, such as cholinergic system dysregulation, metal dyshomeostasis, oxidative stress and amyloid- β ($A\beta$) aggregation, are demonstrated to play important roles in the development of AD, it is difficult to achieve the desirable therapeutic effects by single-target strategy. Therefore, Multi-Target-Directed Ligand (MTDL), which is rationally designed to simultaneously hit multiple targets to improve the pharmacological profiles, has been developed as a promising approach for drug discovery against AD.^[4-6]

To date, most drugs approved for AD are AChE inhibitors, which could improve the level of ACh, an important neurotransmitter responsible for learning, memory, cognition and maintaining consciousness.^[7-8] Besides the reduced ACh level, dyshomeostasis of biometals are also involved in the complex interconnected pathogenesis network of AD. The level of metal ions in AD patients were found to be 3-7 folds higher than healthy individuals,^[9] indicating the dyshomeostasis of biometals (Fe, Cu, Zn) in the brain may contribute to AD pathology.^[10] Moreover, reactive oxygen species (ROS), which leads to oxidative stress and neuronal cell death, are also related to the redox-active metal ions, such as Cu(I) and Fe(II).^[11-14] The phase II clinical trials suggested that clioquinol (CQ), a classic metal chelator used as antifungal drug and antiprotozoal drug, could halt cognitive decline in AD, possibly due to its ability to chelate copper and zinc ions.

Both AChE and metal ions are associated with the aggregation of Amyloid- β ($A\beta$). AChE forms a complex with $A\beta$ and changes the conformation of $A\beta$, therefore promotes the aggregation of $A\beta$.^[15] Metal ions also bind to the histidine residues^[16] of soluble $A\beta$, thus markedly accelerate $A\beta$ nucleated aggregation,^[17,18] an observation enhanced under mild acidic conditions similar to that present in aging and AD brains.^[19] Therefore, simultaneously inhibiting AChE and decreasing metal ions, both of which decelerate the $A\beta$ aggregation through different mechanisms, may render a synergistic effect on the treatment of AD.

Given this, in this study we designed and synthesized a multi-target-directed ligand by

integrating AChE inhibitors and metal chelators, to reduce the hydrolysis of ACh as well as decrease the metal ions levels in brain, therefore inhibit the aggregation of A β . Rivastigmine (Riva), an AChE inhibitor approved for the treatment of AD, was showed to release metabolite NAP226-90 AChE in brain.^[20] Therefore, this compound could be further modified as a multi-target ligand by inhibiting the AChE function and chelating the metal ion via the subsequent hydrolysis products released by AChE. Based on this strategy, quinoline derivatives were designed by conjugating AChE inhibitor Riva with metal chelator CQ. First, we studied the protein binding pattern of one of the typical quinoline derivatives **9b** (Fig. 1) by a molecular docking model described previously,^[21] and found that **9b** had several important interactions with the active-site of AChE in the same mode as Riva. Next, we synthesized 18 quinoline derivatives, and assessed their AChE inhibitory activities, AChE enzymatic metabolites, metal chelating effects and A β aggregation inhibitory activities. The efficacies of the candidate compounds were further evaluated *in vivo* by multiple models.

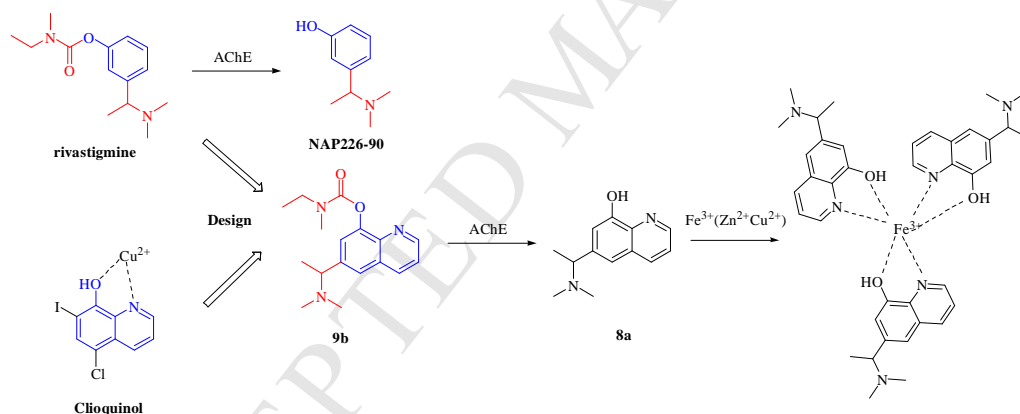


Fig. 1 The design and functions of quinoline derivative **9b**

2. Results and Discussion

2.1 Molecular Docking Study

To understand the molecular interaction between quinoline derivatives and AChE, the molecular docking studies were performed using the Discovery Studio 4.0/CDOCKER protocol.^[21] The crystal structure of Riva/AChE complex (PDB ID: 1GQR) was used as the template. Docking and the subsequent scoring studies were performed using the default parameters. The results showed that the binding patterns of quinoline derivatives in AChE are similar to Riva (Fig. 2). For example, the result of **9b** shows in Fig. 2. Hydrogen bond interactions are observed

between amide group and Gly119/Ser122 with distance of 2.38Å and 2.96Å, respectively. In addition, the quinoline ring forms π - π stacking with Trp84. Moreover, same as the binding pattern of Riva, the carbamate group of **9b** is very close to the esteratic site (Ser200, Glu327 and His440), which is beneficial to hydrolyze the carbamate group and enable a ‘flattening’ of the carbamate moiety over the esteratic site, contributing to the prolonged inhibition of AChE.

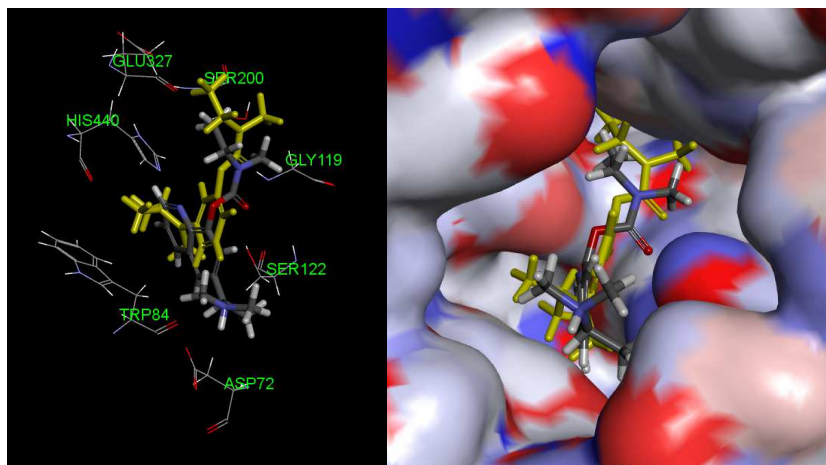


Fig. 2 The molecular docking of rivastigmine (yellow)/**9b** (gray) with AChE

2.2 Chemistry

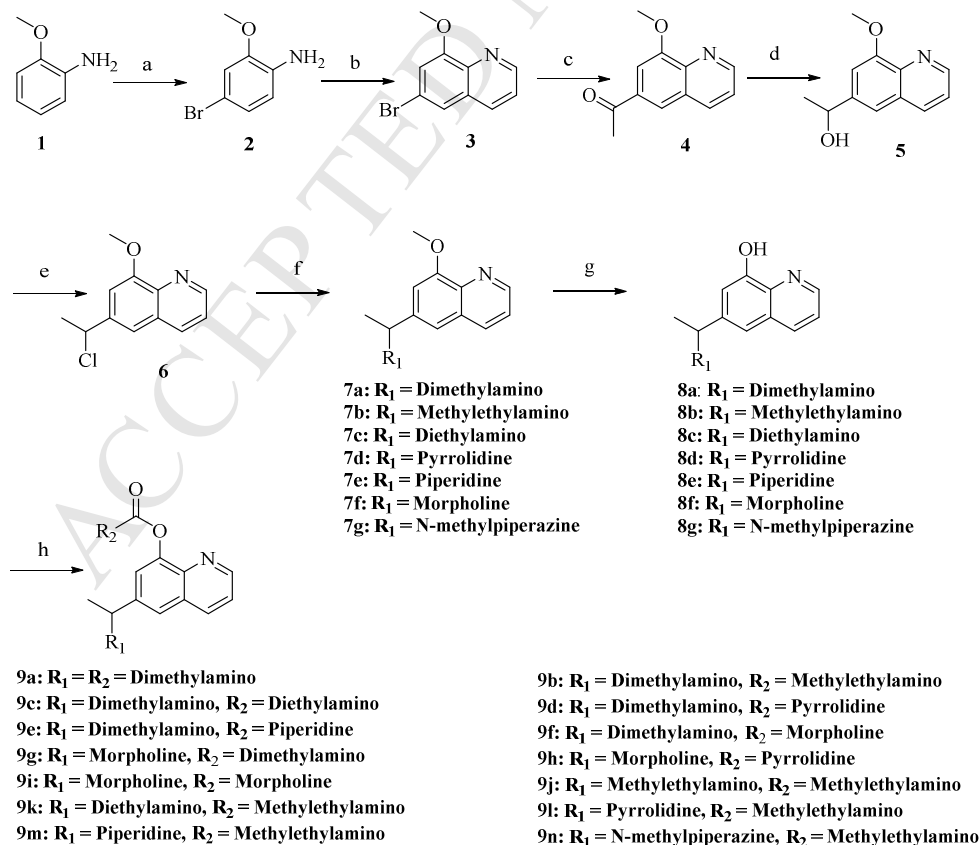


Fig. 3 The synthetic routes of **9a-9n**

Reagents and conditions: (a) Br₂, acetic acid, 0 °C; (b) H₂SO₄, H₂O, nitrobenzene sulfonate, glycerol, reflux; (c) Pd (OAc)₂, DPPP, Et₃N, 1-vinyloxy-butane, 145 °C; (d) NaBH₄, THF, rt; (e) SOCl₂, DCM, rt; (f) R₁H, acetonitrile, reflux; (g) 40% HBr, 130 °C; (h) NaH, R₂COCl, THF, rt.

Quinoline derivatives were prepared according to the procedure depicted in Fig. 3. Reaction of 2-Methoxy-phenylamine with Br₂ afforded compound **2**, which was refluxed with glycerol in H₂SO₄/H₂O and nitrobenzene sulfonate by Skraup reaction to structure the quinoline scaffold. The group Br in compound **3** was substituted by formyl group to yield **4**, followed by reduction of carbonyl group with NaBH₄ to get **5**. The hydroxyl of compound **5** was substituted by chlorine to afford **6**, and then this key intermediate was followed by reaction with various substituted amine to yield **7a-7g**. While treating with HBr led to the loss of methyl group, **8a-8g** were prepared and subsequently acylated with substituted formyl chloride to obtain target compounds **9a-9n**.

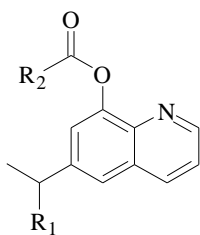
In total, 14 quinoline derivatives (i.e., **9a-9n**) and 7 intermediates (i.e., **8a-8g**), which are the hydrolytic metabolites of **9a-9n**, were designed and synthesized. The chemical structures are shown in Tables 1, and the details of the synthetic procedures and structural characterization are described in the experimental section.

2.3 Biological Activity in vitro

2.3.1 AChE Inhibitory Activity

To evaluate the therapeutic potential of the synthesized quinoline derivatives against AD, **9a-9n** were tested for their AChE inhibition by a modified method of Ellman^[22] using Riva as control (Tab. 1). Among the variations of R² in **9a-9f**, methylethylamino- or morpholine- group demonstrated a significant AChE inhibitory activity. Likewise, the similar SAR was also found in **9g-9i**. Specifically, **9b** displayed the most potent inhibition (IC₅₀: 1.2 ± 0.5 μmol/L, ~7-fold higher than the positive control Riva). With respect to R¹ in **9b** and **9j-9n**, substitution of dimethylamino-group by other aliphatic amino- or various types of alicyclic amino-group remarkably reduced the AChE inhibitory activities. For example, the methylethylamino group at R¹ was 35-fold less potent (**9j** vs **9b**).

Tab. 1 The inhibitions of AChE activity and values of IC₅₀



Compounds	R ¹	R ²	IC ₅₀ (μmol/L)	Compounds	R ¹	R ²	IC ₅₀ (μmol/L)
Rivastigmine	-	-	9.0±2.9	9h			48.6±19.6
9a			16.3±15.1	9i			8.3±3.0
9b			1.2±0.5	9j			40.7±24.6
9c			13.6±3.1	9k			41.2±3.9
9d			28.6±2.1	9l			18.1±3.6
9e			20.6±6.0	9m			29.0±11.7
9f			8.8±0.6	9n			54.7±25.8
9g			69.9±34.0				

2.3.2 Metal Chelating Effect

The metal chelating effect of compound **8a**, a hydrolytic metabolite of **9b**, was investigated using the UV-Vis spectra recorded in methanol at 298K.^[23] As shown in Fig. 4, the absorption was decreased and λ_{max} in the UV-Vis spectra was shifted to red upon the addition of copper ion into **8a**, and the similar shift was observed for the iron/zinc ion. These results are similar with the CQ, which indicated an interaction between **8a** and copper/iron/zinc ion, and **8a** had a potent metal chelating activity. As comparison, compound **9b** had no significant spectral change in the presence of FeSO₄ or CuCl₂, indicating that the formation of metal complex was contributed by the specific interactions between metal ions and the hydroxyl moiety.

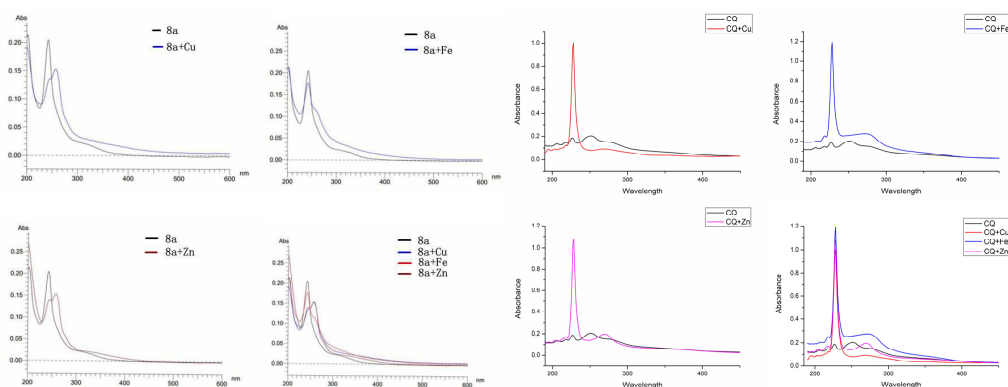


Fig. 4 The absorption spectra of **8a** and **CQ** (25 μ M) chelating with copper, iron and zinc ions

2.3.3 A β Aggregation Inhibition

In order to investigate the A β aggregation inhibition ability of **9b** and **8a**, two methods (TEM and ThT) were used as qualitative and quantitative analyses separately.

2.3.3.1 TEM

The ability of compounds **9b** and **8a** to inhibit A β ₁₋₄₂ self-aggregation was monitored by transmission electron microscopy (TEM) using curcumin as a positive control. After 72h of incubation at 37°C, A β ₁₋₄₂ aggregated into the well-defined amyloid fibrils. In contrast, only a few fibrils could be observed in the presence of curcumin or **9b** or **8a** under the same conditions. Among them, **9b** displayed the most potency in inhibition of aggregation of A β ₁₋₄₂.^[24]

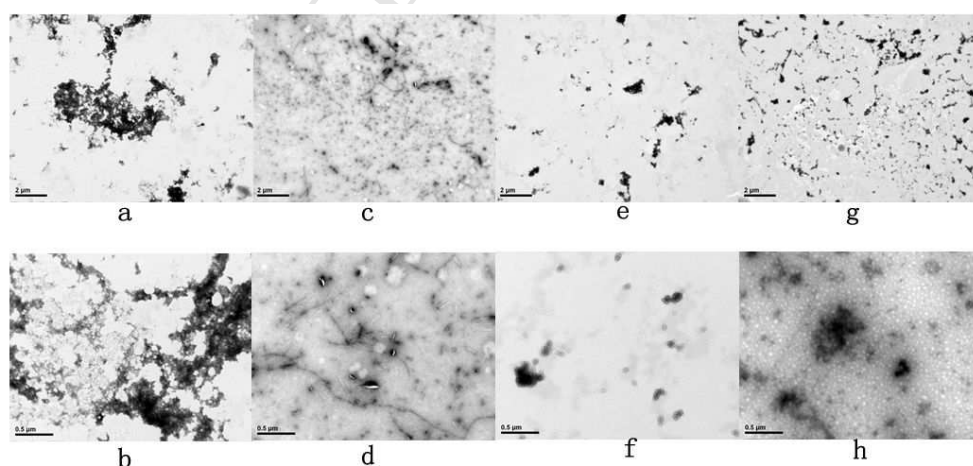


Fig. 5 The transmission electron micrography of A β aggregation inhibition
a/b. A β ; c/d. A β +Cur; e/f. A β +**9b**; g/h. A β +**8a**
(a, c, e and g are 10 000 \times ; b, d, f and h are 50 000 \times)

2.3.3.2 ThT

Thioflavin T (ThT) fluorescence assay was used as quantitative analysis with curcumin as a

reference compound.^[25] As shown in Tab. 2, **9b** demonstrated a marked A β_{1-42} self-aggregation inhibitory activity, presenting more potent inhibition (inhibitory=55.88%) than curcumin (inhibitory=50.19%). Interestingly, the metabolite **8a** also displayed a potent aggregation inhibitory activity. Furthermore, the inhibitory ability of **9b** was at time-dependent manner. Treatment at 24h, **9b** could inhibit 31.34% of A β_{1-42} self-aggregation, while 55.88% at 48h and 66.09% at 72h.

Tab. 2 The results of the ability to inhibit self-induced A β aggregation

Compound	Time	Inhibition%
A β	48h	0
A β +Cur	48h	50.19
A β + 9b	24h	31.34
A β + 9b	48h	55.88
A β + 9b	72h	66.09
A β + 8a	48h	44.05

2.4 Pharmacokinetics *in vitro* and *in vivo*

2.4.1 AChE Enzymatic Hydrolysis Experiments *in vitro*

Carbamate AChE inhibitors such as rivastigmine have been shown to be readily hydrolyzed by AChE with a concomitant release in the brain of the OH metabolite.^[26] In order to study the feasibility of enzymatic removal of the carbamoyl moiety of **9b**, we developed an AChE-mediated hydrolysis model *in vitro*. As shown in Fig. 6, when **9b** was incubated with mouse AChE at 37°C for 12h or 48h, small portion of **8a** could be identified by HPLC after 12h hydrolysis. At 48h, more **9b** was hydrolyzed by AChE to the OH-metabolite **8a**. More interestingly, the OH-metabolite **8a** was the major metabolite of **9b** by AChE.

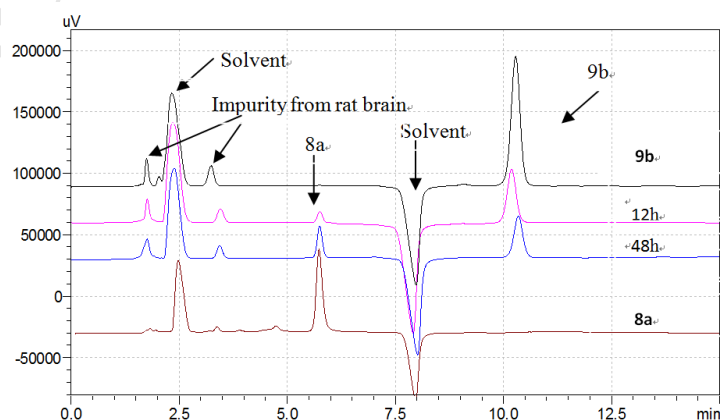


Fig. 6 The HPLC profiles of **9b** and **8a** in the hydrolysis with AChE

2.4.2 Stability Test *in vitro*

Stability of **9b** is critical for crossing the BBB (Blood Brain Barrier) to the brain. Therefore, we assessed the plasma stability, metabolic stability, simulated gastric fluid stability and simulated intestinal fluid stability of **9b**. After incubation with human plasma (from Chempartner), human liver microsomes (from BD Biosciences Gentest), simulated gastric fluid and simulated intestinal fluid respectively, **9b** was measured at 5min, 15min, 30min, 45min and 60min by HPLC. The results in Fig. 7 demonstrated that **9b** is very stable in all the tests.

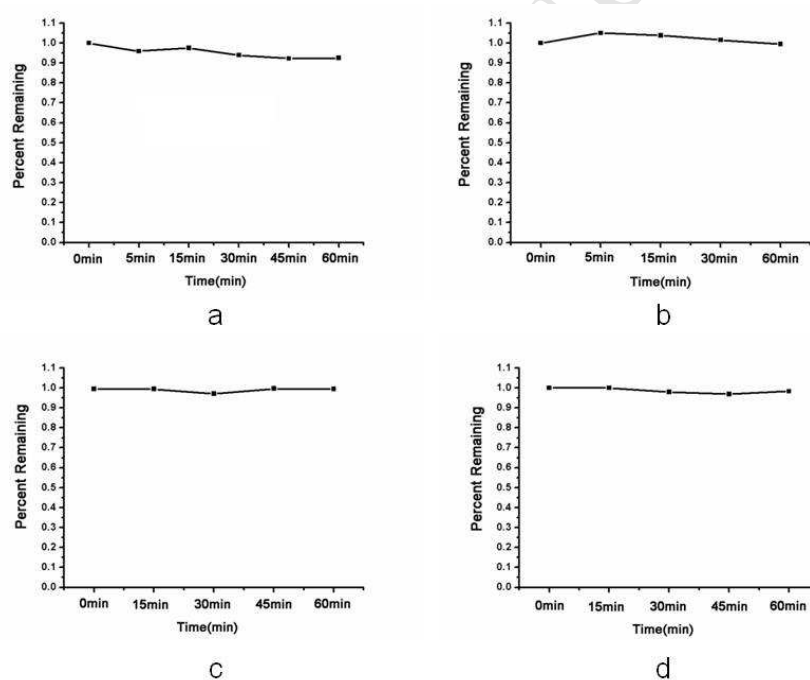


Fig. 7 The stability results of **9b**. a) Plasma stability; b) Metabolic stability; c) Simulated gastric fluid stability; d) Simulated intestinal fluid stability

2.4.3 PK and BBB Penetration of **9b** *in vivo*

BBB penetration is an important factor in the development of MTDL against AD.^[27] To investigate the BBB penetration of **9b**, plasma and brain pharmacokinetic (PK) studies were

performed by microdialysis method.^[28,29] **9b** (25mg/kg) was injected into male Sprague–Dawley rats by intravenous. As shown in Tab. 3, **9b** displayed a high exposure (447.74 ± 149.59 mg/L*min) and extended MRT (91.75 min) in the plasma. More importantly, the brain/plasma exposure ratio was 0.524 (calculated with $AUC_{0-\infty}$ exposure measured for brain and plasma dialysis), indicating that **9b** can efficiently cross the BBB (Fig. 8).

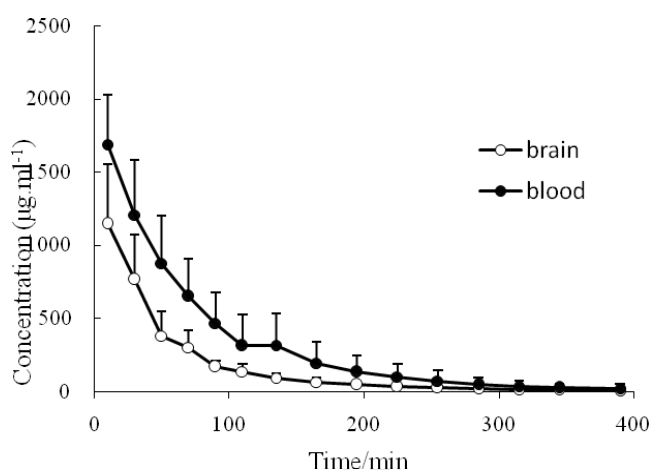


Fig. 8 The pharmacokinetics curve of **9b** in blood dialysis and brain dialysis

Tab.3 The main pharmacokinetic parameters of **9b** in blood dialysis, brain dialysis and plasma of rats. $n=6$, $\bar{x} \pm SD$.

Parameter	9b Plasma	9b Blood dialysis	9b Brain dialysis
AUC_{0-t} (mg/L·min)	444.32 ± 147.815	145.86 ± 50.11	75.69 ± 23.87
$AUC_{0-\infty}$ (mg/L·min)	447.74 ± 149.59	147.16 ± 50.97	76.34 ± 23.38
MRT(min)	91.75 ± 17.07	69.81 ± 20.65	56.82 ± 13.30
CL_z (L/min/kg)	0.062 ± 0.02	0.19 ± 0.08	0.35 ± 0.10

2.5 Cognitive Improvement in Animal Model of AD

2.5.1 Cognitive Improvement in Mice Model of AD

Since there are no animal models available to investigate the target-directed (AChE and metal ion) compound simultaneously, we used two mice models separately, the scopolamine-induced model for targeting AChE, and the Aluminium trichloride-induced model for targeting metal ion,

in which Rivastigmine (Riva, AChE inhibitor) and Clioquinol (CQ, metal chelating agent) were used as positive controls.

The effect of compound **9b** on cognitive improvement was first assessed in a scopolamine (Scop)-induced amnesia animal model. Scop can block the cholinergic pathway by antagonizing the muscarinic receptor, which provides a typical AD model to explore the role of the cholinergic system in cognition and to evaluate anticholinergic drug candidates. In our preliminary experiment, CQ had no effect on cognitive improvement in this model, therefore, we used Riva as the positive control in the following experiment. As shown in Figure 9, the model group exhibited a longer escape latency (63.2 ± 21.1 sec) with a total swimming distance (785 ± 351 cm), as compared to the normal group (36.1 ± 23.5 sec and 445 ± 301 cm). Compound **9b** at 25 mg/kg significantly rescued the escape latency (43.8 ± 17.0 sec) and reduced the total swimming distance (520 ± 168 cm), compared to the model group ($p < 0.05$). The effect of **9b** for the symptom improvement in the *in vivo* model indicated the compound **9b** can be used as a potential anti-AD lead, especially for the treatment of cholinergic deficiency in the early stages of the disease.

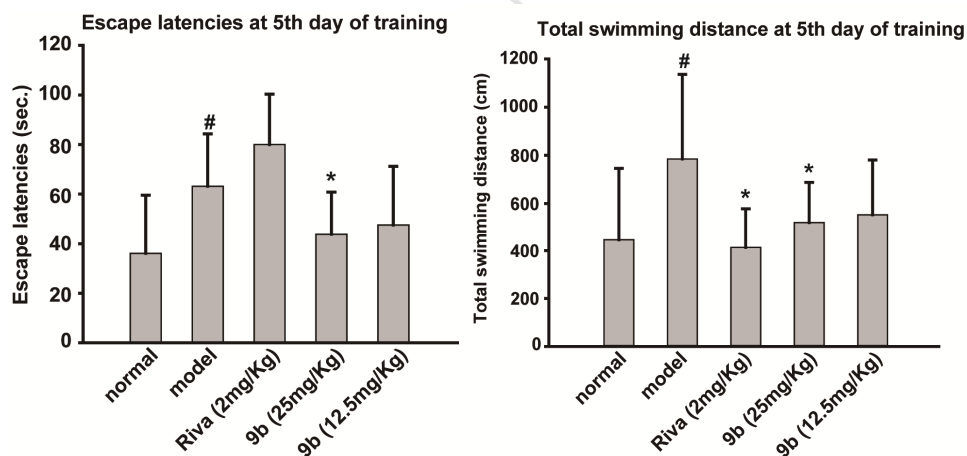


Fig.9 a) The escape latencies at 5th day of training on the Morris water maze; b) The total swimming distance at 5th day of training on the Morris water maze

Next, **9b** was further assessed in an aluminum trichloride-induced amnesia animal model by a SMG-2 programmable water maze using Riva (2mg/kg) and CQ (120mg/kg) as positive control drugs. As shown in Figure 10, the model group exhibited a longer total swimming time (115 ± 19 sec, $p < 0.05$) with more error times (20.7 ± 4.8 sec, $p < 0.05$) than the normal group (66 ± 29 sec and 9.8 ± 5.0 sec). Although the error times for three doses of **9b** didn't show the statistical differences

as compared to the model group, the numbers were still lower with various degrees after the treatment with **9b** (16.8 ± 6.7 at 8mg/kg, 18.1 ± 4.6 at 2mg/kg, 15.1 ± 6.9 at 0.5mg/kg). In addition, upon the treatment of **9b** with 8 mg/kg and 0.5mg/kg, the total swimming times were significantly decreased (79 ± 25 sec at 8mg/kg and 73 ± 29 sec at 0.5mg/kg, $p < 0.05$). The efficacy of **9b** for symptom improvement in this AD mice model also demonstrated its potential anti-AD activity. As comparison, Riva had no effect in this model.

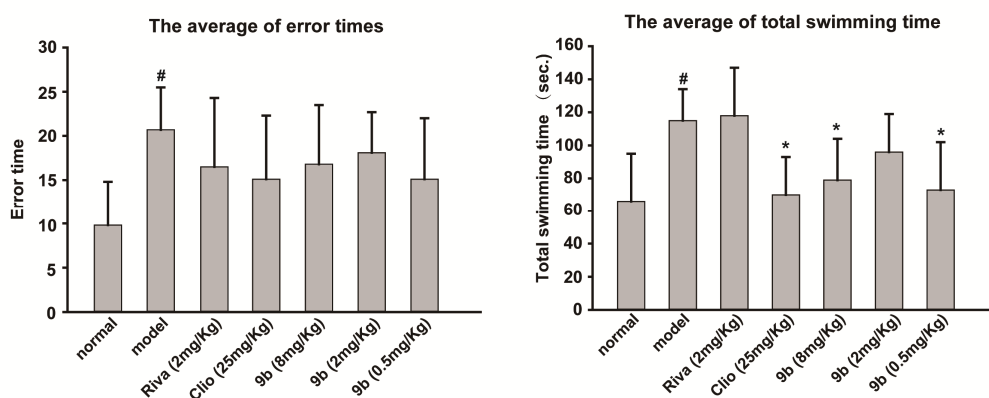


Fig.10 a) The average of error times on the SMG-2 programmable water maze; b) The average time of total swimming time on the SMG-2 programmable water maze

2.5.2 Cognitive Improvement in a Zebrafish Model of AD

The effect of **9b** on cognitive improvement was further assessed in zebrafish model by aluminum chloride exposure, which was previously developed.^[30] We first tested the NOAELs (No Observed Adverse Effect Levels) of **9b**, and then set the high, moderate and low concentrations of **9b** for the efficacy assessment. In the experiment, the zebrafish were first treated with $150 \mu\text{M}$ AlCl_3 from 3 dpf to 5 dpf, and then treated with **9b** at three different doses ($1 \mu\text{M}$, $5 \mu\text{M}$, $25 \mu\text{M}$) from 3 dpf to 5 dpf. Each group had 30 zebrafish. As in the Table 5, the results showed the Dyskinesia Recovery Rate (DRR) measurement was increased in a dose-dependent manner upon **9b** treatment. In addition, the Response Efficiency (RE) measurement was also increased after adding **9b** (Table 4). The effect of **9b** was more significant than rivastigmine, especially in the DRR measurement. The results clearly demonstrated the multi-function of **9b**, i.e. upon penetrating into the brain, **9b** first inhibits acetylcholinesterase, and the hydrolysis product **8a** then acts as a metal chelator.

Table 4 The RE values of six drugs at low, moderate and high concentrations

Drug	Concentration (μM)	DRR%	p	RE %	p
Rivastigmine	10	53.4	0.00298	126.3	0
	50	64.0	0.00012	86.6	0.00004
	250	58.6	0.00310	175.1	0
9b	1	70.8	0.09505	112.4	0.00228
	5	99.3	0.03251	161.4	0.00013
	25	121	0.00329	70.2	0.02818

All the values presented are calculated by the average speed of the drug treated fish.

2.6 Toxicity Evaluation

2.6.1 Cyto-inhibition

To investigate the safety of **9b**, its cytotoxicities on the cell lines Neuro-2a, MCF-7, A549 were studied using a 3-(4,5-dimethylthiazol-2-yl)-2,5-diphenyltetrazolium bromide (MTT) assay.^[25]

The IC_{50} of compound **9b** are $> 20\mu\text{M}$ in all three cell lines, indicating the safety of **9b**.

2.6.2 hERG Inhibition

hERG (the human Ether-à-go-go-Related Gene) is a gene that codes for a protein known as the alpha subunit of a potassium ion channel (sometimes simply denoted as 'hERG'). Since hERG channel mediates the repolarizing IKr current in the cardiac action potential, it can cause a potentially fatal disorder called long QT syndrome when this channel's function is inhibited by application of drugs.^[31] A number of clinically successful drugs in the market had the potential of hERG inhibition, a concomitant risk of sudden death, therefore the hERG inhibition must be avoided for the drug development.^[32] We detected the compound **9b** by patch clamp assay using cisapride as a positive control. The results showed that the IC_{50} of **9b** is $> 30\mu\text{M}$, while the cisapride exhibited 88.99% inhibition at $0.1\mu\text{M}$, indicating that **9b** has a minimal hERG potassium channel inhibition.

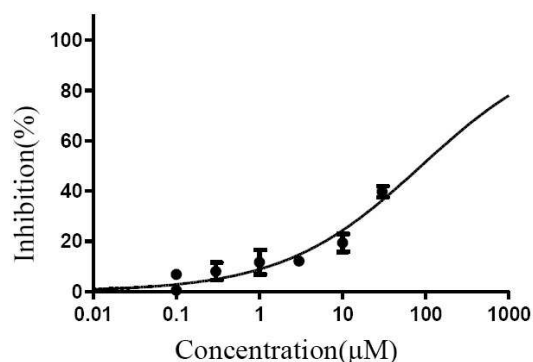


Fig. 11 The hERG inhibition of **9b**

3. Conclusions

Because of the complexity of pathogenesis of AD, a chemical entity against multiple targets might represent a novel therapeutic regimen against AD. In this study we employed the strategy of MTDLs by integrating the AChE inhibitors with the metal chelators, with the goal of not only reducing hydrolysis of ACh thus decreasing the levels of metal ions in brain but also slowing down the aggregation of A β .

Due to the high logP values, most metal chelators can't cross the BBB to the target tissue. We developed a new strategy to "hide" the metal chelator into the AChE inhibitor, which could further release the metal chelator after crossing the BBB by metabolism. The AChE inhibitor, in this case, is not only the anti-AD agent, but also the transporter of the metal chelator. We first showed *in vitro* and *in vivo* that **9b** could cross the BBB, and release **8a** in brain. Furthermore, *in vitro* study found that **9b** has the potent AChE inhibitory activity ($1.2 \pm 0.5 \mu\text{mol/L}$), which is 7-fold more important than rivastigmine. After incubation with AChE, **9b** releases the OH-metabolite **8a**, therefore chelating the metal ions. The A β aggregation inhibition experiments also suggested that both **9b** and **8a** inhibit the A β aggregation.

In vivo, two mice models were used to test **9b** anti-AD activities. Interestingly, both Riva and **9b** are effective on targeting AChE in the scopolamine-induced model, but not CQ. In the aluminum trichloride-induced model, CQ and **9b** are effective on targeting the metal ion, while Riva not. These results indicated that **9b** could reach both targets effectively *in vivo*. The effect of **9b** was further tested in a zebrafish model, showing that **9b** has the cognitive improvement.

In conclusion, our *in vitro* and *in vivo* data demonstrated that **9b** is a potential candidate for AD therapy.

4. Experimental

4.1 General

All solvents used were of analytical grade. Melting points were recorded on a Buchi apparatus and uncorrected. ^1H NMR spectra were recorded on a Bruker Avance III 500M instrument (chemical shifts are expressed as δ values relative to TMS as internal standard). Mass spectra (MS) were recorded on an Esquire-LC-00075 spectrometer. The database of quinoxaline derivatives was built by Pipeline Pilot software.

4.2 Chemistry

Compounds **2**^[33] and **3**^[34] were synthesized according to the known methods.

4.2.1 1-(8-methoxyquinoline-6-yl) acetone (**4**)

Compound **3** (2.4g, 10mmol), $\text{Pd}(\text{OAc})_2$ (110mg, 0.5mmol) and 1,3-Bis(diphenylphosphino)propane (DPPP, 410mg, 1mmol) were dissolved in 20mL alcohol, triethylamine (25mmol) and 1-vinyl-2-butanol (30mmol) were added under nitrogen, and the mixture was refluxed at 150°C for 24h. After cooled to room temperature, 30mL water was added to the mixture, and extracted with dichloromethane (3×30mL). The organic layer was separated and dried over Na_2SO_4 . The solvent was evaporated. The residue was purified by silica gel column chromatography (PE:AcOEt:TEA = 2:1:0.1) to afford **4** as light yellow solid (52%); mp: 64-66°C; ^1H -NMR (δ , CDCl_3): 9.03 (d, 1H, $J = 3.2$ Hz, ArH), 8.26 (d, 1H, $J = 8.0$ Hz, ArH), 8.04 (s, 1H, ArH), 7.64 (s, 1H, ArH), 7.52 (dd, 1H, $J_1 = 8.0$ Hz, $J_2 = 3.2$ Hz, ArH), 4.16 (s, 3H, $-\text{OCH}_3$), 2.75 (s, 3H, $-\text{COCH}_3$). MS(ESI): $m/z = 202$ $[\text{M}+\text{H}]^+$.

4.2.2 1-(8-methoxyquinoline-6-yl) ethanol (**5**)

Compound **4** (1.02g, 5mmol) was dissolved in 50mL THF, NaBH_4 (0.23g, 6mmol) was added by several times. After the mixture was stirred at room temperature for 3h, 50 mL water was added to the mixture, and extracted with ethyl acetate (3×50mL). The organic layer was separated and dried over Na_2SO_4 . The solvent was evaporated and **5** was obtained as light yellow solid (95%);

mp: 51-53 °C; $^1\text{H-NMR}$ (δ , CDCl_3): 8.87 (dd, 1H, $J_1 = 4.4$ Hz, $J_2 = 2.0$ Hz, ArH), 8.07 (dd, 1H, $J_1 = 8.0$ Hz, $J_2 = 2.0$ Hz, ArH), 7.40 (dd, 1H, $J_1 = 8.0$ Hz, $J_2 = 4.4$ Hz, ArH), 7.32 (s, 1H, ArH), 7.09 (s, 1H, ArH), 5.04 (q, 1H, $J = 6.0$ Hz, $-\text{CHOHCH}_3$), 4.84 (s, 1H, $-\text{CHOHCH}_3$), 4.09 (s, 3H, $-\text{OCH}_3$), 1.57 (d, 3H, $J = 6.0$ Hz, $-\text{CHOHCH}_3$). MS(ESI): $m/z = 204$ [M+H] $^+$.

4.2.3 6-(1-chloroethyl)-8-methoxyquinoline (6)

Compound **5** (1.4g, 5mmol) was dissolved in 10mL dichloromethane, 1mL SOCl_2 was added. After the mixture was stirred at room temperature for 12h, 10mL water was added, the organic layer was separated and dried over Na_2SO_4 . The solvent was evaporated and **6** was obtained as light yellow oil (70%); $^1\text{H-NMR}$ (δ , CDCl_3): 9.03 (dd, 1H, $J_1 = 4.4$ Hz, $J_2 = 1.6$ Hz, ArH), 8.12 (dd, 1H, $J_1 = 8.4$ Hz, $J_2 = 1.6$ Hz, ArH), 7.49 (dd, 1H, $J_1 = 8.4$ Hz, $J_2 = 4.4$ Hz, ArH), 7.38 (s, 1H, ArH), 7.13 (s, 1H, ArH), 4.89 (q, 1H, $J = 6.0$ Hz, $-\text{CHClCH}_3$), 3.98 (s, 3H, $-\text{OCH}_3$), 1.64 (d, 3H, $J = 6.0$ Hz, $-\text{CHClCH}_3$). MS(ESI): $m/z = 222$ [M+H] $^+$.

4.2.4 General procedure for the preparation of compounds 7a-g

Compound **6** (0.22g, 1mmol) was dissolved in 5mL acetonitrile, R_1H (5mmol) was added. After the mixture was refluxed for 3h, 10mL water was added, the organic layer was separated and dried over Na_2SO_4 . The solvent was evaporated and **7a-g** was obtained.

4.2.4.1 1-(8-methoxyquinoline-6-yl)-N, N-dimethylamine (7a). Yellow oil (90%); $^1\text{H-NMR}$ (δ , CDCl_3): 8.93 (dd, 1H, $J_1 = 4.4$ Hz, $J_2 = 2.0$ Hz, ArH), 8.07 (dd, 1H, $J_1 = 8.0$ Hz, $J_2 = 2.0$ Hz, ArH), 7.40 (dd, 1H, $J_1 = 8.0$ Hz, $J_2 = 4.4$ Hz, ArH), 7.29 (s, 1H, ArH), 7.16 (s, 1H, ArH), 4.03 (s, 3H, $-\text{OCH}_3$), 3.67 (q, 1H, $J = 6.0$ Hz, $-\text{CHCH}_3$), 2.38 (s, 6H, $-\text{N}(\text{CH}_3)_2$), 1.57 (d, 3H, $J = 6.0$ Hz, $-\text{CHCH}_3$). MS(ESI): $m/z = 231$ [M+H] $^+$.

4.2.4.2 N-ethyl-1-(8-methoxyquinolin-6-yl)-N-methylethan-1-amine (7b). Yellow oil (82%); MS(ESI): $m/z = 245$ [M+H] $^+$.

4.2.4.3 N, N-diethyl-1-(8-methoxyquinolin-6-yl) ethan-1-amine (7c). Yellow oil (88%) ; $^1\text{H-NMR}$ (δ , CDCl_3): 8.98 (s, 1H, ArH), 8.18 (d, 1H, $J = 8.4$ Hz, ArH), 7.52 (dd, 1H, $J_1 = 8.4$ Hz,

$J_2 = 5.6$ Hz, ArH), 7.40 (s, 1H, ArH), 7.22 (s, 1H, $J = 5.6$ Hz, ArH), 4.22 (s, 3H, $-OCH_3$), 4.03 (q, 1H, $J = 6.0$ Hz, $-CHCH_3$), 2.72 (m, 4H, $-N(CH_2CH_3)_2$), 1.53 (d, 3H, $J = 6.0$ Hz, $-CHCH_3$), 1.08 (m, 6H, $-N(CH_2CH_3)_2$). MS(ESI): $m/z = 259$ [M+H]⁺.

4.2.4.4 8-methoxy-6-(1-(pyrrolidin-1-yl) ethyl) quinoline (7d). Yellow oil (85%); MS(ESI): $m/z = 257$ [M+H]⁺.

4.2.4.5 8-methoxy-6-(1-(piperidin-1-yl) ethyl) quinoline (7e). Yellow oil (90%); MS(ESI): $m/z = 271$ [M+H]⁺.

4.2.4.6 4-(1-(8-methoxyquinin-6-yl) ethyl) morpholine (7f). Yellow oil (92%); ¹H-NMR (δ , $CDCl_3$): 8.83 (dd, 1H, $J_1 = 4.0$ Hz, $J_2 = 2.0$ Hz, ArH), 8.00 (dd, 1H, $J_1 = 8.0$ Hz, $J_2 = 2.0$ Hz, ArH), 7.34 (dd, 1H, $J_1 = 8.0$ Hz, $J_2 = 4.0$ Hz, ArH), 7.23 (s, 1H, ArH), 7.11 (s, 1H, ArH), 4.04 (s, 3H, $-OCH_3$), 3.61 (m, 5H, morpholine, $-CHCH_3$), 2.32 (m, 4H, morpholine), 1.57 (d, 3H, $J = 6.4$ Hz, $-CHCH_3$). MS(ESI): $m/z = 273$ [M+H]⁺.

4.2.4.7 8-methoxy-6-(1-(4-methylpiperazin-1-yl) ethyl) quinoline (7g). Yellow oil (90%); MS(ESI): $m/z = 286$ [M+H]⁺.

4.2.5 General procedure for the preparation of compounds 8a-g

Compound **7** (1mmol) was dissolved in 5mL HBr, after the mixture was stirred at 100 °C for 24h, the pH of the mixture was adjusted to 8 by $NaHCO_3$, and extracted with ethyl acetate (3 × 10mL). The organic layer was separated and dried over Na_2SO_4 . The solvent was evaporated and the residue was purified by silica gel column chromatography (PE:AcOEt:TEA = 2:1:0.1) to afford **8**.

4.2.5.1 6-(1-(dimethylamino) ethyl) quinolin-8-ol (8a). Yellow oil (46%); ¹H-NMR (δ , $CDCl_3$): 8.75 (s, 1H, ArH), 8.13 (d, 1H, $J = 8.4$ Hz, ArH), 7.41 (dd, 1H, $J_1 = 8.4$ Hz, $J_2 = 4.0$ Hz, ArH), 7.23 (s, 1H, ArH), 7.13 (d, 1H, $J = 4.0$ Hz, ArH), 3.71 (q, 1H, $J = 6.8$ Hz, $-CHCH_3$), 2.28 (s, 6H, $-N(CH_3)_2$), 1.46 (d, 3H, $J = 6.8$ Hz, $-CHCH_3$). MS(ESI): $m/z = 217$ [M+H]⁺.

4.2.5.2 6-(1-(ethyl(methyl) amido) ethyl) quinolin-8-ol (8b). Brown oil (44%); $^1\text{H-NMR}$ (δ , CDCl_3): 8.73 (d, 1H, $J = 2.8$, ArH), 8.10 (d, 1H, $J = 8.4$ Hz, ArH), 7.40 (dd, 1H, $J_1 = 8.4$ Hz, $J_2 = 2.8$ Hz, ArH), 7.27 (s, 1H, ArH), 7.25 (s, 1H, ArH), 3.68 (q, 1H, $J = 6.4$ Hz, $-\text{CHCH}_3$), 2.42 (q, 2H, $J = 2.8$, $-\text{N}(\text{CH}_3)\text{CH}_2\text{CH}_3$), 2.16 (s, 3H, $-\text{N}(\text{CH}_3)\text{CH}_2\text{CH}_3$), 1.43 (d, 3H, $J = 6.4$ Hz, $-\text{CHCH}_3$), 1.04 (q, 3H, $J = 2.8$, $-\text{N}(\text{CH}_3)\text{CH}_2\text{CH}_3$). MS(ESI): $m/z = 231$ $[\text{M}+\text{H}]^+$.

4.2.5.3 6-(1-(diethylamino) ethyl) quinolin-8-ol (8c). Yellow solid (46%); mp: 65-67 $^\circ\text{C}$; $^1\text{H-NMR}$ (δ , CDCl_3): 8.72 (s, 1H, ArH), 8.11 (d, 1H, $J = 8.4$ Hz, ArH), 7.39 (dd, 1H, $J_1 = 8.4$ Hz, $J_2 = 5.2$ Hz, ArH), 7.32 (s, 1H, ArH), 7.20 (d, 1H, $J = 5.2$ Hz, ArH), 3.91 (q, 1H, $J = 6.0$ Hz, $-\text{CHCH}_3$), 2.57 (m, 4H, $-\text{N}(\text{CH}_2\text{CH}_3)_2$), 1.42 (d, 3H, $J = 6.0$ Hz, $-\text{CHCH}_3$), 1.01 (m, 6H, $-\text{N}(\text{CH}_2\text{CH}_3)_2$). MS(ESI): $m/z = 245$ $[\text{M}+\text{H}]^+$.

4.2.5.4 6-(1-(pyrrolidin-1-yl) ethyl) quinolin-8-ol (8d). Yellow oil (45%); $^1\text{H-NMR}$ (δ , CDCl_3): 8.73 (d, 1H, $J = 4.0$, ArH), 8.08 (d, 1H, $J = 8.0$ Hz, ArH), 7.39 (dd, 1H, $J_1 = 8.0$ Hz, $J_2 = 4.0$ Hz, ArH), 7.30 (s, 1H, ArH), 7.17 (s, 1H, ArH), 3.30 (q, 1H, $J = 6.0$ Hz, $-\text{CHCH}_3$), 2.42 (m, 4H, pyrrolidine), 1.77 (m, 4H, pyrrolidine), 1.46 (d, 3H, $J = 6.0$ Hz, $-\text{CHCH}_3$). MS(ESI): $m/z = 243$ $[\text{M}+\text{H}]^+$.

4.2.5.5 6-(1-(piperidin-1-yl) ethyl) quinolin-8-ol (8e). Light yellow solid (52%); mp: 104-106 $^\circ\text{C}$; $^1\text{H-NMR}$ (δ , CDCl_3): 8.74 (d, 1H, $J = 4.4$, ArH), 8.12 (d, 1H, $J = 8.4$ Hz, ArH), 7.41 (dd, 1H, $J_1 = 8.4$ Hz, $J_2 = 4.4$ Hz, ArH), 7.28 (s, 1H, ArH), 7.25 (s, 1H, ArH), 3.49 (q, 1H, $J = 3.6$ Hz, $-\text{CHCH}_3$), 2.39 (m, 4H, piperidine), 1.55 (m, 4H, piperidine), 1.41 (m, 5H, $-\text{CHCH}_3$, piperidine). MS(ESI): $m/z = 257$ $[\text{M}+\text{H}]^+$.

4.2.5.6 6-(1-morpholinoethyl) quinolin-8-ol (8f). Brown oil (45%); $^1\text{H-NMR}$ (δ , CDCl_3): 8.75 (s, 1H, ArH), 8.12 (d, 1H, $J = 8.4$ Hz, ArH), 7.34 (dd, 1H, $J_1 = 8.4$ Hz, $J_2 = 5.2$ Hz, ArH), 7.28 (s, 1H, ArH), 7.26 (d, 1H, $J = 5.2$ Hz, ArH), 3.72 (m, 4H, morpholine), 3.41 (q, 1H, $J = 6.4$ Hz, $-\text{CHCH}_3$), 2.36 (m, 4H, morpholine), 1.41 (d, 3H, $J = 6.4$ Hz, $-\text{CHCH}_3$). MS(ESI): $m/z = 259$ $[\text{M}+\text{H}]^+$.

4.2.5.7 6-(1-(4-methylpiperazin-1-yl) ethyl) quinolin-8-ol (8g). Yellow solid (45%); mp: 117-119 $^\circ\text{C}$; $^1\text{H-NMR}$ (δ , CDCl_3): 8.72 (d, 1H, $J = 4.0$, ArH), 8.09 (d, 1H, $J = 8.0$ Hz, ArH), 7.40 (dd, 1H, $J_1 = 8.0$ Hz, $J_2 = 4.0$ Hz, ArH), 7.27 (s, 1H, ArH), 7.24 (s, 1H, ArH), 3.44 (q, 1H, $J = 6.4$ Hz, $-\text{CHCH}_3$), 2.47 (m, 8H, 1-methylpiperazine), 2.29 (s, 3H, $-\text{NCH}_3$), 1.40 (d, 3H, $J = 6.4$ Hz, $-\text{CHCH}_3$). MS(ESI): $m/z = 272$ $[\text{M}+\text{H}]^+$.

4.2.6 General procedure for the preparation of compounds 9a-n

Compound **8** (0.5mmol) was dissolved in 10mL THF, NaH (0.6mmol) was added. After the

mixture was stirred at room temperature for 4h, R^2COCl (0.6mmol) was added drop by drop, and the mixture was continued to be stirred at room temperature for 12h. After the solvent was evaporated, 20mL water was added to the mixture, and extracted with ethyl acetate ($3 \times 20mL$). The organic layer was separated and dried over Na_2SO_4 . The solvent was evaporated and the residue was purified by silica gel column chromatography (PE:AcOEt:TEA = 2:1:0.1) to afford **9**.

4.2.6.1 6-(1-(dimethylamino) ethyl) quinolin-8-yl-dimethylcarbamate (9a). Yellow oil (48%); 1H -NMR (δ , $CDCl_3$): 8.90 (d, 1H, $J = 2.8$ Hz, ArH), 8.12 (d, 1H, $J = 8.0$ Hz, ArH), 7.60 (s, 1H, ArH), 7.51 (d, 1H, $J = 8$ Hz, ArH), 7.39 (d, 1H, $J = 4$ Hz, ArH), 3.50 (q, 1H, $J = 6.8$ Hz, $-CHCH_3$), 3.28 (s, 3H, $-CON(CH_3)_2$), 3.07 (s, 3H, $-CON(CH_3)_2$), 2.28 (s, 6H, $-CHN(CH_3)_2$), 1.46 (d, 3H, $J = 6.8$ Hz, $-CHCH_3$). ^{13}C NMR (125 MHz, DMSO- d_6) δ 154.1, 149.2, 147.1, 140.5, 134.9, 128.2, 122.4, 120.6, 64.6, 41.9, 35.9, 28.7, 18.5. HRMS (ESI) m/z Calcd $C_{16}H_{22}N_3O_2$ (M+H) 288.1712, found 288.1715.

4.2.6.2 6-(1-(dimethylamino) ethyl) quinolin-8-yl ethyl(methyl)carbamate (9b). Brown oil (51%); 1H -NMR (δ , $CDCl_3$): 8.91-8.90 (d, 1H, $J = 4.0$ Hz, ArH), 8.15-8.12 (d, 1H, $J = 12.0$ Hz, ArH), 7.60 (s, 1H, ArH), 7.52-7.53 (d, 1H, $J = 4.0$ Hz, ArH), 7.41-7.38 (dd, 1H, $J_1 = 8.0$ Hz, $J_2 = 4.0$ Hz, ArH), 3.71-3.66 (m, 1H, $-NCH_2CH_3$), 3.46-3.52 (m, 2H, $-NCH_2CH_3$), 3.27 (s, 1.5H, $-NCH_3$), 3.07 (s, 1.5H, $-NCH_3$), 2.28 (s, 6H, $-NCH_3$), 1.48 (d, 3H, $J = 4.0$ Hz, $-CHCH_3$), 1.38 (m, 1.5H, $-NCH_2CH_3$), 1.25 (m, 1.5H, $-NCH_2CH_3$). ^{13}C NMR (125 MHz, DMSO- d_6) δ 154.7, 145.0, 148.2, 143.1, 141.4, 135.9, 129.1, 123.2, 121.5, 65.5, 44.4, 43.2, 34.2, 19.9, 13.1. HRMS (ESI) m/z Calcd $C_{17}H_{24}N_3O_2$ (M+H) 302.1869, found 302.1880.

4.2.6.3 6-(1-(dimethylamino) ethyl) quinolin-8-yl diethylcarbamate (9c). Yellow oil (58%); 1H -NMR (δ , DMSO- d_6): 8.87 (d, 1H, $J = 4.0$ Hz, ArH), 8.11 (d, 1H, $J = 8.4$ Hz, ArH), 7.57 (dd, 1H, $J_1 = 8.4$ Hz, $J_2 = 4.0$ Hz, ArH), 7.52 (s, 1H, ArH), 7.36 (d, 1H, $J = 4.0$ Hz, ArH), 3.66 (q, 2H, $J = 7.2$ Hz, $-NCH_2CH_3$), 3.40 (m, 3H, $-CHN(CH_3)_2$, $-NCH_2CH_3$), 2.26 (s, 6H, $-CHN(CH_3)_2$), 1.46 (d, 3H, $J = 6.4$ Hz, $-CHCH_3$), 1.38 (t, 2H, $J = 7.2$ Hz, $-CHCH_3$), 1.26 (t, 4H, $J = 7.2$ Hz, $-CHCH_3$). ^{13}C NMR (125 MHz, DMSO- d_6) δ 154.6, 149.8, 148.2, 142.7, 141.6, 135.6, 129.4, 123.0, 121.5, 65.5, 43.2, 42.3, 29.7, 20.0, 14.5, 13.4. HRMS (ESI) m/z Calcd $C_{18}H_{26}N_3O_2$ (M+H) 316.2025, found 316.2031.

4.2.6.4 6-(1-(dimethylamino) ethyl) quinolin-8-yl pyrrolidine-1-carboxylate (9d). Brown oil (41%); 1H -NMR (δ , $CDCl_3$): 8.91 (d, 1H, $J = 4.0$ Hz, ArH), 8.14 (d, 1H, $J = 8.0$ Hz, ArH), 7.61 (s, 1H, ArH), 7.54 (s, 1H, ArH), 7.38 (d, 1H, $J = 8.0$ Hz, ArH), 3.81 (t, 1H, $J = 6.0$ Hz, $-CHN(CH_3)_2$), 3.52-3.56 (m, 4H, pyrrolidine), 2.27 (s, 6H, $-CHN(CH_3)_2$), 1.42 (t, 3H, $J = 6.0$ Hz, $-CHCH_3$), 1.23 (m, 4H, pyrrolidine). ^{13}C NMR (125 MHz, DMSO- d_6) δ 155.5, 149.8, 143.0, 135.5, 129.0, 121.6, 111.4, 101.0, 66.4, 36.2, 47.9, 43.3, 25.7, 20.1. HRMS (ESI) m/z Calcd $C_{18}H_{24}N_3O_2$ (M+H) 314.1869, found 314.1870.

4.2.6.5 6-(1-(dimethylamino) ethyl) quinolin-8-yl piperidine-1-carboxylate (9e). Brown oil (46%); 1H -NMR (δ , $CDCl_3$): 8.89 (d, 1H, $J = 6.8$ Hz, ArH), 8.12 (d, 1H, $J = 8.4$ Hz, ArH), 7.57 (s, 1H, ArH), 7.51 (s, 1H, ArH), 7.40 (m, 1H, ArH), 3.81-3.56 (m, 4H, piperidine), 3.45-3.40 (t, 1H, $J =$

6.0 Hz, $-CHN(CH_3)_2$), 2.26(s, 6H, $-CHN(CH_3)_2$), 1.69(s, 6H, pyridine), 1.44 (d, 3H, $J = 6.8$ Hz, $-CHCH_3$). ^{13}C NMR (125 MHz, DMSO- d_6) δ 154.0, 149.8, 148.4, 143.0, 141.4, 135.8, 129.2, 122.9, 121.5, 65.6, 46.0, 45.3, 43.2, 29.6, 25.9. HRMS (ESI) m/z Calcd $C_{19}H_{26}N_3O_2$ (M+H) 328.2025, found 328.2028.

4.2.6.6 6-(1-(dimethylamino) ethyl) quinolin-8-yl morpholine-4-carboxylate (9f). Yellow oil (59%); 1H -NMR (δ , $CDCl_3$): 8.91 (d, 1H, $J = 4.4$ Hz, ArH), 8.12 (d, 1H, $J = 8.4$ Hz, ArH), 7.60(dd, 1H, $J_1 = 8.4$ Hz, $J_2 = 4.4$ Hz, ArH), 7.55 (d, 1H, $J = 1.6$ Hz, ArH), 7.41 (d, 1H, $J = 1.6$ Hz, ArH), 3.73 (s, 4H, morphine), 3.50 (m, 1H, $J = 4.8$ Hz, $-CHN(CH_3)_2$), 3.21(s, 3H, $-CHN(CH_3)_2$), 3.09 (s, 3H, $-CHN(CH_3)_2$), 2.57-2.44(m, 4H, morphine) 1.44 (d, 3H, $J = 6.4$ Hz, $-CHCH_3$). ^{13}C NMR (125 MHz, DMSO- d_6) δ 154.5, 147.8, 142.6, 138.8, 134.8, 128.1, 120.7, 116.4, 106.1, 65.6, 55.0, 46.2, 42.7, 28.7, 19.4, 16.6. HRMS (ESI) m/z Calcd $C_{18}H_{24}N_3O_3$ (M+H) 330.1818, found 330.1823.

4.2.6.7 6-(1-morpholinoethyl) quinolin-8-yl dimethylcarbamate (9g). Orange oil (42%); 1H -NMR (δ , $CDCl_3$): 8.90(d, 1H, $J = 4.4$ Hz, ArH), 8.12(d, 1H, $J = 8.0$ Hz, ArH), 7.60 (s, 1H, ArH), 7.55 (d, 1H, $J = 8.0$ Hz, ArH), 7.40 (d, 1H, $J_2 = 4.0$ Hz, ArH), 3.72 (m, 4H, morpholine), 3.50 (q, 1H, $J = 5.6$ Hz, $-CHCH_3$), 3.31 (s, 3H, $-NCH_3$), 3.09(s, 3H, $-NCH_3$), 2.44-2.57 (m, 4H, morpholine), 1.45 (d, 3H, $J = 5.6$ Hz, $-CHCH_3$). ^{13}C NMR (125 MHz, DMSO- d_6) δ 155.1, 150.0, 148.0, 142.7, 141.4, 135.8, 129.2, 123.3, 121.6, 121.5, 67.0, 65.0, 51.2, 36.8, 29.7, 19.4. HRMS (ESI) m/z Calcd $C_{18}H_{24}N_3O_3$ (M+H) 330.1818, found 330.1829.

4.2.6.8 6-(1-morpholinoethyl) quinolin-8-yl pyrrolidine-1-carboxylate (9h). Brown oil (43%); 1H -NMR (δ , $CDCl_3$): 8.92 (d, 1H, $J = 2.4$ Hz, ArH), 8.15 (d, 1H, $J = 8.4$ Hz, ArH), 7.61 (s, 1H, ArH), 7.43 (dd, 1H, $J_1 = 8.4$ Hz, $J_2 = 2.4$ Hz, ArH), 7.30 (s, 1H, ArH), 4.14 (m, 2H, pyrrolidine), 3.82 (m, 1H, pyrrolidine), 3.74 (m, 4H, morpholine), 3.56 (m, 1H, pyrrolidine), 3.57(m, 1H, $-CHCH_3$), 2.57-2.45 (m, 4H, morpholine), 2.00 (m, 4H, pyrrolidine), 1.45 (m, 3H, $-CHCH_3$). ^{13}C NMR (125 MHz, DMSO- d_6) δ 154.58, 149.0, 146.9, 140.4, 134.7, 128.2, 122.1, 120.8, 116.7, 109.5, 66.1, 64.0, 55.1, 50.5, 45.6, 28.7, 24.8, 24.0, 13.2. HRMS (ESI) m/z Calcd $C_{20}H_{26}N_3O_3$ (M+H) 356.1974, found 356.1987.

4.2.6.9 6-(1-morpholinoethyl) quinolin-8-yl morpholine-4-carboxylate (9i). Yellow oil (61%); 1H -NMR (δ , $CDCl_3$): 8.88 (d, 1H, $J = 4$ Hz, ArH), 8.11 (d, 1H, $J = 8.4$ Hz, ArH), 7.60 (s, 1H, ArH), 7.55 (s, 1H, ArH), 7.40 (m, 1H, ArH), 3.88-3.83 (m, 6H, morpholine), 3.71-3.64 (m, 6H, morpholine), 3.50 (q, 1H, $J = 6.4$ Hz, $-CHCH_3$), 2.55-2.44 (m, 4H, morpholine), 1.41 (d, 3H, $J = 6.4$ Hz, $-CHCH_3$). ^{13}C NMR (125 MHz, DMSO- d_6) δ 154.1, 150.0, 148.0, 141.2, 135.8, 129.2, 123.5, 121.7, 121.3, 67.1, 66.6, 65.0, 51.3, 45.5, 44.5, 29.7, 19.5. HRMS (ESI) m/z Calcd $C_{20}H_{26}N_3O_4$ (M+H) 372.1923, found 372.1930.

4.2.6.10 6-(1-(ethyl (methyl) amino) ethyl) quinolin-8-yl ethyl (methyl) carbamate (9j). Yellow oil (55%); 1H -NMR (δ , $CDCl_3$): 8.91 (d, 1H, $J = 3.6$ Hz, ArH), 8.10 (d, 1H, $J = 8.4$ Hz, ArH), 7.43 (dd, 1H, $J_1 = 8.4$ Hz, $J_2 = 3.6$ Hz, ArH), 7.30 (s, 1H, ArH), 7.24 (s, 1H, ArH), 4.14 (m, 3.5H, $-CONCH_3$, $-CONCH_2CH_3$), 3.71 (m, 1.5H, $-CONCH_3$), 3.50 (m, 1H, $-CHCH_3$), 2.58 (m, 2H,

-NCH₂CH₃), 2.33 (s, 3H, -NCH₃), 1.50 (d, 3H, *J* = 6 Hz, -CHCH₃), 1.26 (m, 3H, -CONCH₂CH₃), 1.10 (m, 3H, -NCH₂CH₃). ¹³C NMR (125 MHz, DMSO-*d*₆) δ 153.9, 148.8, 146.9, 142.7, 140.3, 134.7, 128.1, 121.8, 121.1, 120.4, 59.4, 43.4, 41.9, 20.1, 13.1, 11.1. HRMS (ESI) *m/z* Calcd C₁₈H₂₆N₃O₂ (M+H) 316.2025, found 316.2031.

4.2.6.11 6-(1-(diethylamino) ethyl) quinolin-8-yl ethyl (methyl) carbamate (9k). Yellow oil (54%); ¹H-NMR (δ , CDCl₃): 8.89 (d, 1H, *J* = 4.0 Hz, ArH), 8.12 (d, 1H, *J* = 8.0 Hz, ArH), 7.43 (s, 1H, ArH), 7.30 (d, 1H, *J* = 6.8 Hz, ArH), 7.20 (dd, 1H, *J*₁ = 8.0 Hz, *J*₂ = 6.8 Hz, ArH), 4.15 (d, 4H, *J* = 6.0 Hz, -CONCH₃, -CONCH₂CH₃), 3.37 (m, 2H, -CHCH₃, -CONCH₂CH₃), 2.55 (s, 2H, -NCH₂CH₃), 2.45 (s, 2H, -NCH₂CH₃), 2.05 (s, 2H, -CHNCH₂CH₃), 1.82 (s, 4H, -CHNCH₂CH₃), 1.52 (d, 3H, *J* = 6.0 Hz, -CHCH₃), 1.28 (m, 3H, -CONCH₂CH₃). ¹³C NMR (125 MHz, DMSO-*d*₆) δ 154.9, 154.8, 149.6, 147.9, 144.1, 141.3, 135.6, 129.1, 122.6, 122.0, 121.3, 58.7, 45.0, 42.9, 35.6, 34.2, 17.1, 13.1, 12.3. HRMS (ESI) *m/z* Calcd C₁₉H₂₈N₃O₂ (M+H) 330.2182, found 330.2187.

4.2.6.12 6-(1-(pyrrolidin-1-yl) ethyl) quinolin-8-yl ethyl (methyl) carbamate (9l). Yellow oil (52%); ¹H-NMR (δ , CDCl₃): 8.89 (d, 1H, *J* = 4.0 Hz, ArH), 8.10 (d, 1H, *J* = 8.8 Hz, ArH), 7.63 (dd, 1H, *J*₁ = 8.8 Hz, *J*₂ = 4.0 Hz, ArH), 7.30 (s, 1H, ArH), 7.20 (s, 1H, ArH), 4.15 (s, 5H, -NCH₃, -NCH₂CH₃), 3.37 (q, 1H, *J* = 5.6 Hz, -CHCH₃), 2.65-2.47 (m, 4H, pyrrolidine), 1.82 (m, 4H, pyrrolidine), 1.52 (d, 3H, *J* = 5.6 Hz, -CHCH₃), 1.28 (t, 3H, *J* = 6.8 Hz, -NCH₃). MS(ESI): *m/z* = 328 [M+H]⁺. ¹³C NMR (125 MHz, DMSO-*d*₆) δ 151.4, 149.1, 147.1, 141.6, 140.4, 134.8, 128.4, 121.3, 120.6, 120.3, 64.9, 59.3, 52.1, 43.5, 37.7, 33.15, 22.4, 12.21, 11.53. HRMS (ESI) *m/z* Calcd C₁₉H₂₆N₃O₂ (M+H) 328.2025, found 328.2027.

4.2.6.13 6-(1-(piperidin-1-yl) ethyl) quinolin-8-yl ethyl (methyl) carbamate (9m). Yellow oil (57%); ¹H-NMR (δ , CDCl₃): 8.87 (d, 1H, *J* = 3.8 Hz, ArH), 8.10 (d, 1H, *J* = 8.3 Hz, ArH), 7.57 (s, 1H, ArH), 7.53 (d, 1H, *J* = 6.8 Hz, ArH), 7.37 (dd, 1H, *J*₁ = 8.2 Hz, *J*₂ = 4.1 Hz, ArH), 3.68 (q, 1H, *J* = 6.8 Hz, -NCHCH₃), 3.56 (q, 1H, *J* = 6.8 Hz, -NCH₂CH₃), 3.48 (dd, 1H, *J*₁ = 13.9 Hz, *J*₂ = 6.8 Hz, -NCH₂CH₃), 3.26 (s, 1.5H, -NCH₃), 3.06 (s, 1.5H, -NCH₃), 2.41 (m, 4H, piperidine), 1.57 (m, 4H, piperidine), 1.44 (d, 3H, *J* = 6.8 Hz, -CHCH₃), 1.39 (m, 3.5H, piperidine, -CH₂CH₃), 1.25 (t, 1.5H, *J* = 6.8 Hz, -CH₂CH₃). ¹³C NMR (125 MHz, DMSO-*d*₆) δ 154.8, 149.9, 147.9, 142.6, 141.3, 135.8, 129.2, 123.2, 121.9, 121.5, 64.9, 51.6, 44.5, 34.3, 29.7, 26.1, 24.5, 18.9, 13.2, 12.5. HRMS (ESI) *m/z* Calcd C₂₀H₂₈N₃O₂ (M+H) 342.2182, found 342.2188.

4.2.6.14 6-(1-(4-methylpiperazin-1-yl) ethyl) quinolin-8-yl ethyl (methyl) carbamate (9n). Yellow oil (40%); ¹H-NMR (δ , CDCl₃): 8.88 (d, 1H, *J* = 3.2 Hz, ArH), 8.12 (d, 1H, *J* = 8 Hz, ArH), 7.58 (s, 1H, ArH), 7.53 (d, 1H, *J* = 8 Hz, ArH), 7.39 (dd, 1H, *J*₁ = 8.0 Hz, *J*₂ = 3.2 Hz, ArH), 4.13 (q, 1H, *J* = 6.8 Hz, -CHCH₃), 3.67 (q, 1H, *J* = 7.2 Hz, -NCH₂CH₃), 3.27 (m, 2.5H, -CONCH₃, -NCH₂CH₃), 3.06 (s, 1.5H, -CONCH₃), 2.51 (m, 8H, 1-Methyl-piperazine), 2.32 (s, 3H, -NCH₃),

1.43 (d, 3H, $J = 6.8$ Hz, $-\text{CHCH}_3$), 1.41 (t, 1.5H, $J = 7.2$ Hz, $-\text{NCH}_2\text{CH}_3$), 1.12 (t, 1.5H, $J = 7.2$ Hz, $-\text{NCH}_2\text{CH}_3$). ^{13}C NMR (125 MHz, $\text{DMSO}-d_6$) δ 154.7, 149.9, 148.0, 142.7, 141.44, 135.7, 129.2, 123.2, 121.4, 64.4, 55.4, 50.2, 45.5, 44.5, 44.0, 34.3, 19.6, 13.2, 12.4. HRMS (ESI) m/z Calcd $\text{C}_{20}\text{H}_{29}\text{N}_4\text{O}_2$ (M+H) 357.2291, found 357.2300.

Acknowledgments

This work was supported by Natural Science Foundation of Zhejiang Province (LY17H310008 and LQ17H300003), Health Commission of Zhejiang Province (XKQ-010-001, WJK-ZJ-1918 and 2019KY365), and the State Key Laboratory of Medicinal Chemical Biology.

Authors' contributions

Wenhai Huang designed the study, and drafted the manuscript; Meihao Liang, Chixiao Zhang, Beibei Wang and Zhimin Zhang performed chemistry; Li Tang performed $\text{A}\beta$ Aggregation Inhibition; Qiao Wang performed PK; Qin Li and Xiaoliang Zheng performed animal models; Zhengrong Shen revised the manuscript; All authors read and approved the final manuscript.

Competing interests

The authors declare that they have no competing interests.

List of abbreviations:

AChE:acetylcholinesterase
 $\text{A}\beta$:amyloid- β
BBB: Blood Brain Barrier
AD:Alzheimer's disease
ACh:acetylcholine
MTDL:Multi-Target-Directed Ligand
Riva:Rivastigmine
TEM:transmission electron microscopy
ThT:Thioflavin T
PK:pharmacokinetic
MRT:Mean Retention Time
AUC:Area Under Curve
CQ:Clioquinol
Scop:scopolamine
No Observed Adverse Effect Levels:NOAELs
DRR:Dyskinesia Recovery Rate

RE:Response Efficiency
hERG:the human Ether-à-go-go-Related Gene

References and notes

- [1] Latta, C. H.; Brothers, H. M.; Wilcock, D. M. Neuroinflammation in Alzheimer's disease: A source of heterogeneity and target for personalized therapy. *Neuroscience*. **2014**, *5*, S0306-4522.
- [2] Behl, C. The search for novel avenues for the therapy and prevention of Alzheimer's disease. *Drug News Perspect*. **2006**, *19*, 5-12.
- [3] Cummings, J. L.; Morstorf, T.; Zhong, K. Alzheimer's disease drug-development pipeline: few candidates, frequent failures. *Alzheimer's Research & Therapy*. **2014**, *6*, 37.
- [4] Morphy, R.; Rankovic, Z. Designed multiple ligands. An emerging drug discovery paradigm. *J. Med. Chem*. **2005**, *48*, 6523-6543.
- [5] Prati, F.; Bergamini, C.; Fato, R.; Soukup, O.; Korabecny, J.; Andrisano, V.; Bartolini, M.; Bolognesi M. L. Novel 8-Hydroxyquinoline Derivatives as Multitarget Compounds for the Treatment of Alzheimer's Disease. *ChemMedChem*. **2016**, *11*, 1284-1295.
- [6] Chalupova, K.; Korabecny, J.; Bartolini, M.; Monti, B.; Lamba, D.; Caliandro, R.; Pesaresi, A.; Brazzolotto, X.; Gastellier, A. J.; Nachon, F.; Pejchal, J.; Jarosova, M.; Hepnarova, V.; Jun, D.; Hrabanova, M.; Dolezal, R.; Zdarova, K. J.; Mzik, M.; Kristofikova, Z.; Misik, J.; Muckova, L.; Jost, P.; Soukup, O.; Benkova, M.; Setnicka, V.; Habartova, L.; Chvojkova, M.; Kleteckova, L.; Vales, K.; Mezeiova, E.; Uliassi, E.; Valis, M.; Nepovimova, E.; Bolognesi, M. L.; Kuca, K. Novel tacrine-tryptophan hybrids: Multi-target directed ligands as potential treatment for Alzheimer's disease. *Eur J Med Chem*. **2019**, *168*, 491-514.
- [7] Bartus, R. T.; Dean, R. L., 3rd; Beer, B.; Lippa, A. S. The cholinergic hypothesis of geriatric memory dysfunction. *Science*. **1982**, *217*, 408-414.
- [8] Perry, E.; Walker, M.; Grace, J.; Perry, R. Acetylcholine in mind: a neurotransmitter correlate of consciousness? *Trends Neurosci*. **1999**, *22*, 273-280.
- [9] Zatta, P.; Drago, D.; Bolognin, S.; Sensi, S. L. Alzheimer's disease, metal ions and metal homeostatic therapy. *Trends Pharmacol Sci*. **2009**, *30*, 346-355.
- [10] Lovell, M. A.; Robertson, J. D.; Teesdale, W. J.; Campbell, J. L.; Markesbery, W. R. Copper, iron and zinc in Alzheimer's disease senile plaques. *J Neurol Sci*. **1998**, *158*, 47-52.
- [11] Lee, H. J.; Korshavn, K. J.; Kochi, A.; Derrick, J. S.; Lim, M. H. Cholesterol and metal ions in Alzheimer's disease. *Chem. Soc. Rev*. **2014**, *43*, 6672-6682.
- [12] Savelieff, M. G.; DeToma, A. S.; Derrick, J. S.; Lim, M. H. The ongoing search for small molecules to study metal-associated amyloid- β species in Alzheimer's disease. *Acc. Chem. Res*. **2014**, *47*, 2475-2482.
- [13] Duce, J. A.; Bush, A. I. Biological metals and Alzheimer's disease: Implications for therapeutics and diagnostics. *Prog. Neurobiol. (Oxford, U. K.)* **2010**, *92*, 1-18.

- [14] Ayton, S.; Lei, P.; Bush, A. I. Metallostasis in Alzheimer's disease. *Free Radical Biol. Med.* **2013**, *62*, 76–89.
- [15] Inestrosa, N. C.; Dinamarca, M. C.; Alvarez, A. Amyloid-cholinesterase interactions. *FEBS J.* **2008**, *275*, 625-632.
- [16] Bush, A. I. Drug development based on the metals hypothesis of Alzheimer's disease. *J. Alzheimer's Dis.* **2008**, *15*, 223-240.
- [17] Raffa, D. F.; Gomez-Balderas, R.; Brunelle, P.; Rickard, G. A.; Rauk, A. A β initio model studies of copper β binding to peptides containing a His-His sequence: relevance to the beta-amyloid peptide of Alzheimer's disease. *J. Biol. Inorg. Chem.* **2005**, *10*, 8872-8902.
- [18] Faller, P. Copper in Alzheimer disease: too much, too little, or misplaced? *Free Radic. Bio. Med.* **2012**, *52*, 747-748.
- [19] Srinivas, N. R. Transdermal Rivastigmine delivery for Alzheimer disease: Amenability of exposure predictions of rivastigmine and metabolite, NAP226-90, by linear regression model using limited samples. *Clin. Neuropharmacol.* **2016**, *39*, 169-177.
- [20] Inestrosa, N. C.; Alvarez, A.; Dinamarca, M. C.; Pérez-Acle, T.; Colombres, M. Acetylcholinesterase-amyloid- β -peptide interaction: effect of Congo Red and the role of the Wnt pathway. *Curr. Alzheimer Res.* **2005**, *2*, 301-306.
- [21] Huang, W.-H.; Tang, L.; Shi, Y.; Huang, S.-F.; Xu, L.; Sheng, R.; Wu, P.; Li, J.; Zhou, N.-M.; Hu, Y.-Z. Searching for the multi-target-directed ligands against Alzheimer's disease: Discovery of quinoxaline-based hybrid compounds with AChE, H3R, and BACE 1 inhibitory activities. *Bioorg Med Chem.* **2011**, *19*, 7158-7167.
- [22] Ellman, G. L.; Courtney, K. D.; Andres jr, V.; Featherstone, R. M. A new and rapid colorimetric determination of acetylcholinesterase activity. *Biochem. Pharmacol.* **1961**, *7*, 88-95.
- [23] Huang, W.-H.; Lv, D.; Yu, H.-P.; Sheng, R.; Kim, S. C.; Wu, P.; Luo, K.-D.; Li, J.; Hu, Y.-Z. Dual-target-directed 1,3-diphenylurea derivatives: BACE 1 inhibitor and metal chelator against Alzheimer's disease. *Bioorg Med Chem.* **2010**, *18*, 5610-5615.
- [24] Rosini, M.; Simoni, E.; Bartolini, M.; Cavalli, A.; Ceccarini, L.; Pascu, N.; McClymont, D. W.; Tarozzi, A.; Bolognesi, M. L.; Minarini, A.; Tumiatti, V.; Andrisano, V.; Mellor, I. R.; Melchiorre, C. Inhibition of acetylcholinesterase, β -amyloid aggregation, and NMDR receptors in Alzheimer's disease: a promising direction for the multi-target-directed ligands gold rush. *J. Med. Chem.* **2008**, *51*, 4381–4384.
- [25] Sheng, R.; Tang, L.; Jiang, L.; Hong, L.-J.; Shi, Y.; Zhou, N. -M.; Hu, Y.-Z. Novel 1-Phenyl-3-hydroxy-4-pyridinone derivatives as multifunctional agents for the therapy of Alzheimer's disease. *Acs Chemical Neuroscience.* **2016**, *7*, 69.
- [26] Bar-On, P.; Millard, C. B.; Harel, M.; Dvir, H.; Enz, A.; Sussman, J. L.; Silman, I. Kinetic and structural studies on the interaction of cholinesterases with the anti-Alzheimer drug rivastigmine. *Biochemistry.* **2002**, *41*, 3555-3564.

- [27] Bolea, I.; Gella, A.; Unzeta, M. Propargylaminederived multitarget-directed ligands: fighting Alzheimer's disease with monoamine oxidase inhibitors. *J. Neural Transm.* **2013**, *120*, 893–902.
- [28] Tang, L.-N.; Zhang, Y.-W.; Wang, S.-H. Liver, blood microdialysate and plasma pharmacokinetics of matrine following transdermal or intravenous administration. *Pharmazie.* **2017**, *72*, 167–170.
- [29] Wang, Q.; Tang, Z.; Zhang W.-G. Brain microdialysate, CSF and plasma pharmacokinetics of ligustrazine hydrochloride in rats after intranasal and intravenous administration. *Biopharmaceutics & Drug Disposition.* **2013**, *34*, 417-422.
- [30] Huang, W.-H.; Li, C.-S.; Shen, Z.-R.; Zhu, X.-Y.; Xia, B.; Li, C.-Q. Development of a Zebrafish Model for Rapid Drug Screening against Alzheimer's Disease. *Journal of Pharmacy and Pharmacology.* **2016**, *4*, 174-185.
- [31] Hedley, P.L.; Jørgensen, P.; Schlamowitz, S.; Wangari, R.; Moolman-Smook, J.; Brink, P. A.; Kanters, J. K.; Corfield, V. A.; Christiansen, M. The genetic basis of long QT and short QT syndromes: a mutation update. *Hum. Mutat.* **2009**, *30*, 1486–511.
- [32] Sanguinetti, M. C.; Tristani-Firouzi, M. hERG potassium channels and cardiac arrhythmia. *Nature.* **2006**, *440*, 463–9.
- [33] Kohn, M. Bromination of o-Acetanisidide, o-Anisidine, and a molecular rearrangement in the bromination of 4,5-dibromo-o-anisidine. *Journal of Organic Chemistry,* **1953**, *18*, 530-533.
- [34] Zhang, L.-L.; Eric Meggers. An Extremely Stable and Orthogonal DNA-Base Pair with a Three-Carbon Backbone. *Journal of American Chemical Society,* **2005**, *127*, 74-75.

A total of 18 quinoline derivatives were synthesized. Both *in vitro* and *in vivo* results demonstrated that compound **9b** could cross BBB, then release **8a** into brain. **9b** could inhibit AChE, while **8a** displayed metal ion chelating function, therefore in combination, both **9b** and **8a** exhibited a considerable inhibition of A β aggregation, one of the observations that plays important roles in the pathogenesis of AD. The efficacy of **9b** against AD was further investigated in both a zebrafish model and two different mice models.